Journal of Instrumentation

Radiation imaging with optically read out GEM-based detectors

Jinst

Published by IOP Publishing for Sissa Medialab

Received: *January 15, 2018*
Accepted: *February 7, 2018*
Published: *February 19, 2018*

TECHNICAL REPORT

Radiation imaging with optically read out GEM-based detectors

F.M. Brunbauer,[a,b,1] **M. Lupberger,**[a] **E. Oliveri,**[a] **F. Resnati,**[a] **L. Ropelewski,**[a] **C. Streli,**[b] **P. Thuiner**[a] **and M. van Stenis**[a]

[a] *CERN,*
385 Route de Meyrin, 1217 Meyrin, Geneva, Switzerland
[b] *Technische Universität Wien,*
Karlsplatz 13, 1040 Wien, Wien, Austria

E-mail: florian.brunbauer@cern.ch

Abstract: Modern imaging sensors allow for high granularity optical readout of radiation detectors such as MicroPattern Gaseous Detectors (MPGDs). Taking advantage of the high signal amplification factors achievable by MPGD technologies such as Gaseous Electron Multipliers (GEMs), highly sensitive detectors can be realised and employing gas mixtures with strong scintillation yield in the visible wavelength regime, optical readout of such detectors can provide high-resolution event representations. Applications from X-ray imaging to fluoroscopy and tomography profit from the good spatial resolution of optical readout and the possibility to obtain images without the need for extensive reconstruction. Sensitivity to low-energy X-rays and energy resolution permit energy resolved imaging and material distinction in X-ray fluorescence measurements. Additionally, the low material budget of gaseous detectors and the possibility to couple scintillation light to imaging sensors via fibres or mirrors makes optically read out GEMs an ideal candidate for beam monitoring detectors in high energy physics as well as radiotherapy. We present applications and achievements of optically read out GEM-based detectors including high spatial resolution imaging and X-ray fluorescence measurements as an alternative readout approach for MPGDs. A detector concept for low intensity applications such as X-ray crystallography, which maximises detection efficiency with a thick conversion region but mitigates parallax-induced broadening is presented and beam monitoring capabilities of optical readout are explored. Augmenting high resolution 2D projections of particle tracks obtained with optical readout with timing information from fast photon detectors or transparent anodes for charge readout, 3D reconstruction of particle trajectories can be performed and permits the realisation of optically read out time projection chambers. Combining readily available high performance imaging sensors with compatible scintillating gases and the strong signal amplification factors achieved by MPGDs makes optical readout an attractive alternative

[1] Corresponding author.

https://doi.org/10.1088/1748-0221/13/02/T02006

2018 JINST 13 T02006

to the common concept of electronic readout of radiation detectors. Outstanding signal-to-noise ratios and robustness against electronic noise allow unprecedented imaging capabilities for various applications in fields ranging from high energy physics to medical instrumentation.

KEYWORDS: Gaseous imaging and tracking detectors; Micropattern gaseous detectors (MSGC, GEM, THGEM, RETHGEM, MHSP, MICROPIC, MICROMEGAS, InGrid, etc); Optical detector readout concepts; X-ray detectors

2018 JINST 13 T02006

Contents

2018 JINST 13 T02006

1 Introduction

Ranging from particle or photon counting to position and energy sensitive imaging, radiation detection is of crucial importance for numerous fields including high energy physics, radiation protection, industrial material analysis and medical physics, to name but a few. Depending on these applications, detectors have to fulfill requirements of sensitivity, spatial and temporal resolution and accuracy in addition to radiation hardness, material budget limits and other technical constraints. Relying on state-of-the-art manufacturing techniques, MicroPattern Gaseous Detectors (MPGDs) are able to meet the most stringent requirements of high energy physics experiments [1] and have also achieved popularity in medical imaging [2, 3] and neutron detection and beam monitoring [4, 5]. After converting incident radiation to primary electrons through ionization of the gas in a drift volume acting as active target, MPGDs employ high electric field regions to achieve high charge multiplication factors in electron avalanche processes. The inherent micrometer-scale structures in MPGD technologies such as Gaseous Electron Multipliers (GEMs) [6] and the operation of such detectors in a proportional amplification regime allow for high position resolution as well as energy resolved detection. Commonly, MPGDs are read out by either collecting amplified electrical charge on an anode or by recording induced electrical signals in readout strips or pads, which are capacitively coupled to an anode plane. While readout pads or crossed readout strips allow for position resolved reconstruction, the required signal processing effort to extract images from individual analogue signal pulses can be significant. Additionally, electronic readout of MPGDs is highly sensitive to electronic noise and careful circuit and readout geometry design has to be employed to minimize the destructive influence of electronic noise.

While electronic readout relies on collecting charge or detecting induced signal from moving electrons, optical readout of the scintillation light produced during avalanche multiplication in high electric field regions in gaseous detectors presents an alternative readout approach for MPGDs. Inherently insensitive to electronic noise, optical readout relies on the emission of scintillation light during de-excitation processes of gas atoms or molecules after ionization events [7]. In many cases, the produced scintillation light is in the UV-range and requires UV-sensitive photon detectors or wavelength shifters to record. However, some gas mixtures, most notably CF_4-based mixtures,

exhibit scintillation light spectra with a strong photon yield in the visible wavelength regime [8] and can be readily used for direct detection with imaging sensors of CCD or CMOS cameras. Modern imaging sensors feature very low readout noise values allowing sensitivity to small light signals and a high number of pixels providing high spatial resolution in the read out images. Optical readout allows for a prompt display of visual representations of radiation events, as there is no need for extensive image reconstruction, and is thus ideally suited for online radiation monitoring applications in the fields of radiation protection or beam monitoring. The high spatial resolution due to the high granularity provided by imaging sensors coupled with the strong signal amplification permitted by MPGDs allows for sensitive 2D detectors based on optical readout which provide accurate and high-resolution position information. This can be of particular interest in nuclear physics experiments studying rare events [9] as well as in directional dark matter search [10].

2 Optical readout of GEMs

Optical readout of GEM-based detectors relies on the detection of emitted scintillation light following electron avalanche multiplication in the high electric field regions inside the holes of the GEM [11]. While sufficiently high electric fields are able to accelerate electrons strongly enough to trigger subsequent ionisation processes in the gas and lead to a release of additional free electrons, the ionised gas atoms and molecules remain in excited states in many cases. When transitioning from these excited states to their respective ground states, they can emit the excess energy as scintillation photons. This scintillation light is termed primary scintillation light if it is emitted as a result of initial ionisation events in the conversion volume of MPGD-based detectors or secondary scintillation light if emitted during avalanche charge multiplication in high electric field regions.

The low intensity of primary scintillation light produced in the conversion volume requires highly sensitive photon detectors such as Photomultiplier Tubes (PMTs) for efficient detection, while modern imaging sensor as used in CCD or CMOS cameras can be employed for recording the much higher intensity secondary scintillation light signals. However, high light yield alone is not sufficient for camera-based readout of detectors as the emitted scintillation light spectra often feature strong UV-components, which conventional imaging sensors are not sensitive for. While wavelength shifters may be used for converting scintillation in the UV-range to visible light, certain gases inherently feature scintillation light spectra with copious photon flux in the visible wavelength regime. Most popularly, CF_4 features a strong visible scintillation light peak [7] around 620 nm and allows for direct readout of scintillation light with state-of-the-art imaging sensors. The secondary scintillation light spectrum of an Ar/CF_4 (80/20% by volume) gas mixture in the visible wavelength range is shown in figure 1 and compared to the quantum efficiency curve of a commercially available CCD imaging sensor.

The overall amount of photons emitted during charge multiplication is proportional to the number of generated electrons during avalanche processes in the holes of the GEM operating at fixed gain. Therefore, the energy of the incident radiation interacting in the conversion volume of the detector is reflected in the number of emitted scintillation photons and allows for energy resolved imaging based on optically read out GEMs.

Optical readout relies on sufficiently strong scintillation to be recorded by CCD or CMOS imaging sensors. The scintillation light yield, i.e. the number of photons emitted per electron in the electron avalanches, of a GEM-based detector can be used as a quantitative measure for a

2018 JINST 13 T02006

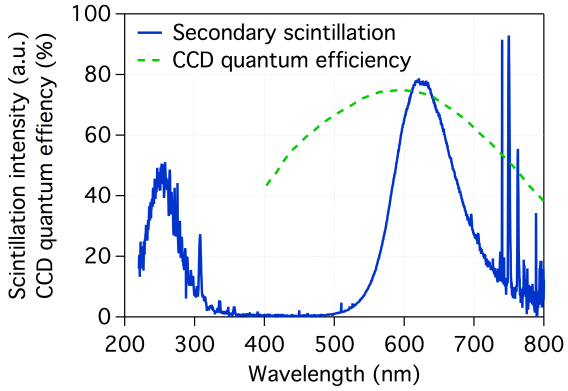

Figure 1. Secondary scintillation spectrum of Ar/CF_4 (80/20%) mixture exhibiting strong scintillation in the visible wavelength regime. The shown quantum efficiency curve of a commercially available CCD camera [12] overlaps with the peak of the Ar/CF_4 scintillation spectrum.

comparison of the amount of scintillation light produced when operating at different charge gains or in different operating regimes such as varying gas mixtures or pressures. To allow for high charge multiplication factors and consequently high light yield while still operating the detector in a stable regime, multiple GEMs can be operated in series [6].

Besides a dependence on GEM voltage, scintillation light yield is also highly dependent on impurities in the gas filling of the detectors with minimal amounts of contaminants significantly decreasing light production. Operating detectors in open gas flow ensures constant gas purity despite possible outgassing from detector components. Alternatively, UHV-grade vessels in combination with detector elements built from materials selected for their low outgassing rates can be employed for optically read out detectors operating in sealed mode.

Taking advantage of readily available CCD or CMOS imaging sensors, high granularity optical readout of GEM-based detectors is possible. Sensitive sensors with several megapixels with low read noise at the level of a few electrons can be used to achieve sensitivity to low light signals while simultaneously enabling long exposure times. We present GEM-based radiation detection and imaging detectors read out with a 6 megapixel CCD camera with a $12.5 \times 10\,\mathrm{mm}^2$ cooled imaging sensor featuring $4.54 \times 4.54\,\mu\mathrm{m}^2$ pixels with a read noise below six electrons [12]. Coupled to a triple-GEM detector with an active area of $10 \times 10\,\mathrm{cm}^2$ with a large aperture lens, such a camera allows for high-resolution imaging applications.

The employed triple-GEM detector is powered with a resistor divider applying a voltage difference of 400 V across each GEM layer. A comparable voltage drop across the 2 mm transfer regions between the GEMs results in transfer fields of 2 kV/cm. A drift region with a thickness of 5 mm between the top GEM electrode and the cathode was used. No anode below the GEM stack was used in order to collect all electrons on the bottom of the last GEM and allow for scintillation light readout. The CCD camera was facing the bottom electrode of the third GEM and focused on the surface of the GEM with a 25 mm lens with an additional +3 diopter lens in front of it. With a distance of approximately 25 cm between the lens of the camera and the GEM, the full active area could be recorded by the imaging sensor, which corresponds to a magnification factor of 10. The optical readout setup for imaging applications is schematically shown in figure 2a. An image of the employed triple-GEM detector housed inside of a transparent gas volume is shown in figure 2b.

2018 JINST 13 T02006

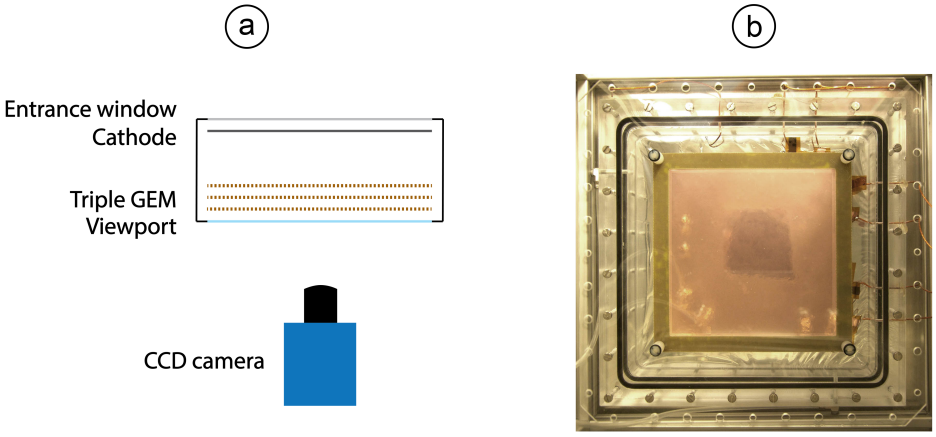

Figure 2. (a) Schematic of the optical readout setup consisting of a triple-GEM inside of a transparent gas volume read out by a CCD camera. (b) Image of the triple-GEM detector with $10 \times 10\,\mathrm{cm}^2$ active area housed inside of an optically transparent gas volume.

3 Applications

3.1 Radiography

The high spatial resolution achievable with optical readout makes it an attractive readout concept for MPGDs in imaging applications. Since cameras directly provide displayable images, no extensive image reconstruction algorithms are necessary and obtaining visual representations of incident radiation is both fast and simple. To correct for variations in gain of the triple-GEM multiplication stage across the active area, a flood exposure with uniform incident X-rays is performed and acquired images are normalised to the obtained gain map. Additionally, a background image without irradiation is acquired and subtracted from acquired images to correct for any possible offset in the grayscale values from the camera.

Placing an object of interest in front of the radiation entrance window of a detector and irradiation with a flat X-ray photon field, X-ray radiographs can be recorded. The high signal amplification of GEM-based detectors enables imaging even with low energetic X-rays such as 5.9 keV ^{55}Fe or 8 keV Cu X-rays. A radiograph of a deceased bat recorded with an exposure time of 30 s under irradiation with Cu X-rays is shown in figure 3a, while a radiograph of a miniature drone is shown in figure 3b.

The contrast in the images allows distinguishing different material densities in the obtained X-ray radiographs. The high position resolution allows the identification of individual GEM holes as the sources of scintillation light. The hexagonal pattern of the 70 µm diameter GEM holes with a pitch of 140 µm is clearly visible in the optically read out images as shown in the inset of figure 3a.

Due to the low readout noise and dark current of the employed CCD imaging sensors, the signal-to-noise ratio of radiographs can be increased with longer exposure times or increased irradiation rate. While in static imaging applications longer exposure times can be used to improve the contrast of the radiographs, CCD or CMOS cameras allow for recording images at rates of tens of images per second, which can be used to record X-ray fluoroscopy movies. Under sufficiently strong irradiation, even optically read out images with exposure times of fractions of a second allow

2018 JINST 13 T02006

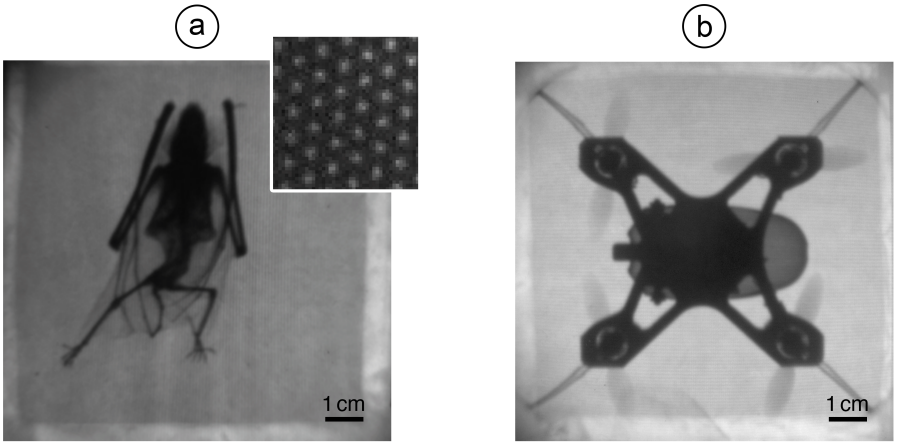

Figure 3. (a) Optically read out X-ray radiograph of a small mammal. The bone structure of the bat is clearly visible. Inset: the holes of the GEM are visible as sources of scintillation light. (b) Radiograph of a miniature drone.

for unambiguous distinction of geometric features. This can be used to record real-time moving radiographs, which can be of importance in functional radiology or non-invasive online material characterisation in industrial applications. The fluoroscopy capabilities of the presented detector have been demonstrated by a real-time recording of a remote controlled miniature drone flying between an X-ray tube and the optically read out detector as well as a fluoroscopy recording of a working wall clock.

Capturing radiographs of an object from multiple angles, 3D reconstruction can be performed. Radiographs capturing projections of a rotating crushed plastic cup containing two pens permit a reconstruction of the 3D object by computing sinograms and performing a filtered back projection. An exemplary projection of the object is shown in figure 4a along with a 3D view of the obtained reconstruction in figure 4b.

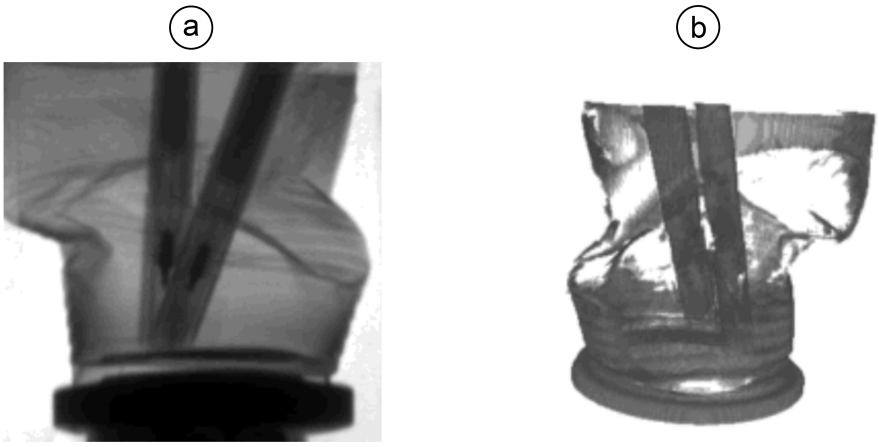

Figure 4. (a) Projection of a crushed plastic cup containing two pens. (b) 3D reconstructed model of the object obtained from computed sinograms and filtered back projection.

2018 JINST 13 T02006

3.2 X-ray fluorescence

Energy resolved X-ray imaging enables material distinction by distinguishing characteristic energy X-ray emission from different materials. Energy resolved detectors sensitive to single low energy X-ray photons can be realised with the high charge gains provided by multi-layer GEM amplification structures and read out optically.

The amount of light produced during electron avalanches in the GEM multiplication structure is proportional to the number of electrons produced in the amplification process and therefore proportional to the energy released by the initial incident radiation in the drift region. Operating a triple-GEM detector at high gain, secondary scintillation light from single low energy X-ray photons interacting in the active volume of the detector can be unambiguously identified in optically read out images with short exposure times as shown in figure 5a.

By integrating the pixel values in a circular region centred on each individual X-ray photon signal spot, the energy of the incident photon can be determined. Recording the energy of many of these signals and binning them by energy, an energy spectrum of the incident radiation can be built up in the same way as when integrating the charge recorded by electronic readout. A comparison of an ^{55}Fe energy spectrum obtained from integrating electronic signals on the bottom of the last GEM in a triple GEM stack (figure 5b) with an energy spectrum obtained from pixel value integration of individual X-ray photons in optically read out images (figure 5c) demonstrates the possibility of energy resolved imaging. The double peak structure displays a dominant full energy peak corresponding to an X-ray energy of 5.9 keV as well as a less abundant escape peak at 2.9 keV. The energy resolution in the case of the ^{55}Fe energy spectrum obtained with optical readout is 32% FWHM at 5.9 keV.

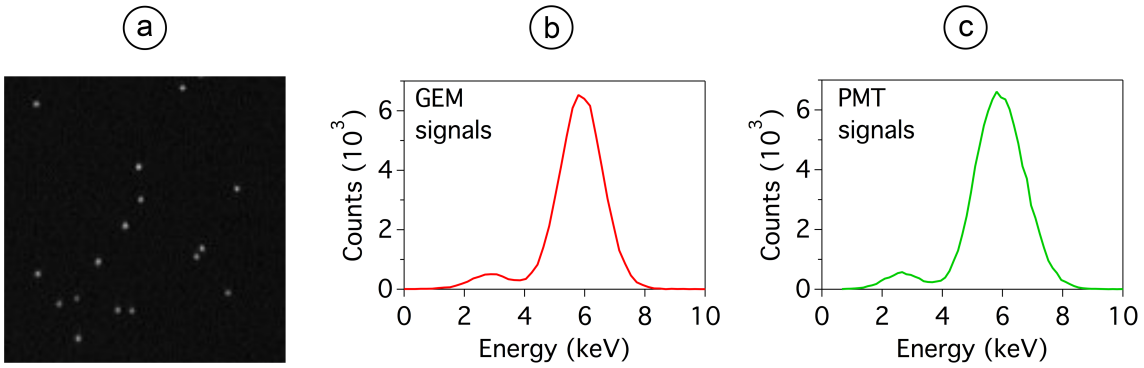

Figure 5. (a) Individual ^{55}Fe X-ray photons visible in optically read out image. (b) ^{55}Fe X-ray energy spectrum acquired by electronically reading out charge pulses on the bottom electrode of the last GEM. (c) ^{55}Fe X-ray energy spectrum acquired by integrating the intensity of individual X-ray photon spots in optically read out images.

Recording both the energy and the location of individual X-ray photon signal spots, energy resolved images could be reconstructed from a high number of photon interaction events. This X-ray fluorescence technique can be applied to identify different materials in an image. An experimental setup to demonstrate this capability consisting of an object containing different materials irradiated with 20 keV X-rays and a pinhole placed between the object and an optically read out GEM-based detector is shown in figure 6a. The ambient light image of the examined object containing different materials is shown in figure 6b.

2018 JINST 13 T02006

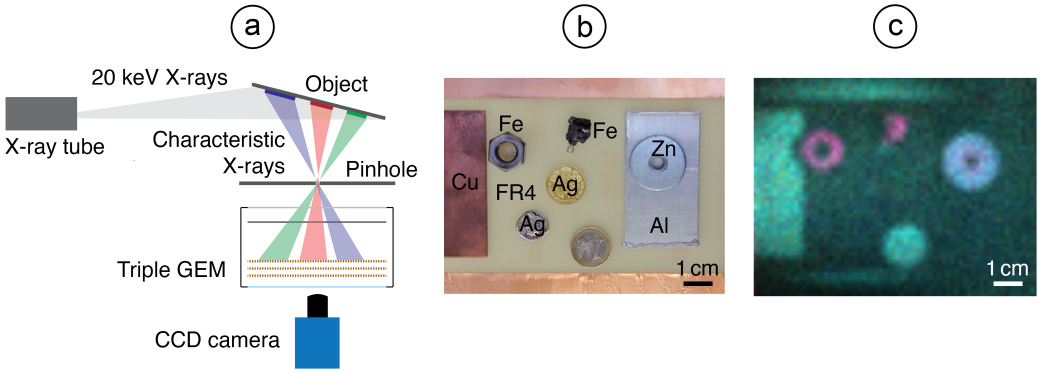

Figure 6. (a) X-ray fluorescence setup with pinhole and optically read out GEM-based detector. (b) Visible light image of investigated object containing different materials. (c) Energy-resolved color-coded image. Different colours correspond to different materials: Cu: green, Fe: pink, Zn: blue. The higher energetic characteristic X-ray emission from Au could not be induced. The low energy Al fluorescence photons could not traverse the radiation window of the detector.

Materials are excited by the incident X-rays and characteristic X-ray emission is induced. The X-rays are focused through the pinhole onto the detector and detected by recording signal energy and location in short exposure images obtained with a CCD camera. Subsequently, a false-color image as shown in figure 6c is reconstructed with the color-coding representing the energies of the recorded X-ray photons. This allows for a spatially resolved distinction and identification of different materials across the $10 \times 10\,\mathrm{cm}^2$ active area of the detector.

The decreased efficiency of gaseous detectors for higher energetic X-rays due to the absorption length in the active medium may limit their applicability for low photon flux applications such as X-ray fluoroscopy or crystallography. Increasing the interaction and subsequently the detection probability of X-rays in gaseous detectors by increasing the thickness of the active drift region, parallax-induced broadening results in a loss of position resolution and signal-to-noise ratio. For non-parallel X-rays originating from a point-like source, the uncertainty in interaction depth in the drift region will lead to a broadening of signals which limits detector performance in fluorescence and crystallography applications. Drift field lines radially focused on a point-like radiation source can be used to minimise the parallax error. While previous designs employing spherical GEMs [13] to achieve radially focused drift fields were not ideally suited for optical readout, segmented cathode and GEM electrodes biased at different potentials can be used to maintain a flat detector geometry while achieving radially focused drift field lines [14]. Such a planispherical GEM detector is well suited for X-ray fluorescence and crystallography and enables the preservation of the high position resolution in applications requiring thick drift regions for increased radiation detection efficiency.

3.3 Radiation imaging and event reconstruction

An intuitive way of obtaining visual representations of events in the active detection volume combined with high granularity make optical readout ideally suited for imaging applications extending from X-ray radiographs to identifying and investigating a wide range of radiation types. The strong signal amplification provided by multi-layer GEM structures enables tuneable detector sensitivity from minimum ionizing particles (MIPs) and low-energy X-rays up to highly ionising radiation like alpha particles.

2018 JINST 13 T02006

The optically read out triple-GEM detector was operated in a muon beam with the beam parallel to the GEMs and aimed at a 10 mm thick drift volume. Operating the GEMs at high gain and reading out with 8×8 pixel binning with an exposure time of 1 ms to minimise event pileup, individual muon tracks could be recorded as shown in figure 7a. The characteristic cluster structure along the otherwise straight muon tracks can be observed along with the occasional emission of delta-rays from the muon tracks as shown in figure 7b.

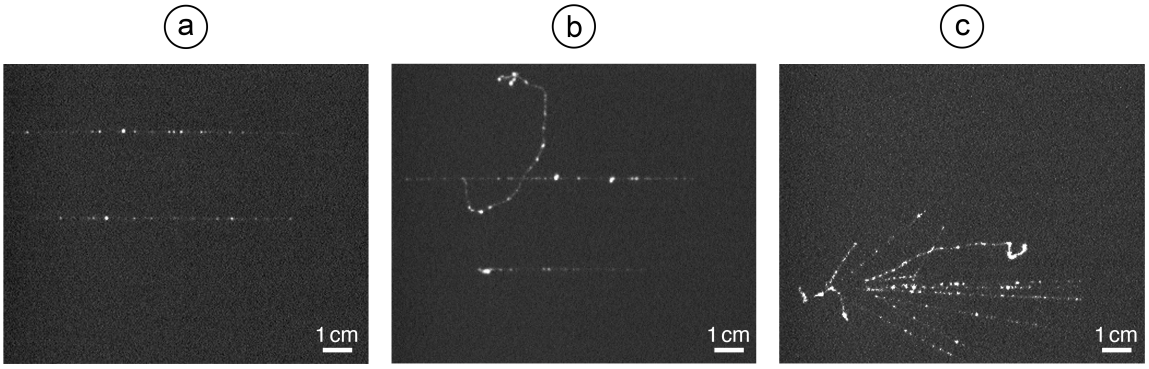

Figure 7. (a) Muon tracks with cluster structure. (b) Delta-ray emitted from muon traversing the active region. (c) Hadronic shower with numerous particle tracks originating from a single location.

The low and uniform background level can be subtracted to allow for a determination of the released energy from the integrated intensity of the pixels in the images. The immediate onscreen display of the images from the camera without the need for extensive reconstruction permits a prompt identification and categorisation of events and can be used to clearly distinguish muon tracks from delta-rays or hadronic shower events as shown in figure 7c.

In the case of highly ionising particles, excellent signal-to-noise ratios can be obtained and energy loss profiles along tracks can be extracted from images along with the origin and orientation of particle trajectories. An image of an alpha track from the decay of ^{220}Rn to ^{216}Po recorded with an optically read out GEM-based detector is shown in figure 8a. ^{216}Po decays again via alpha decay to ^{212}Pb with a short half life of 145 ms and with sufficiently long exposure times both of these alpha decays can be captured within the same image as shown in figure 8b.

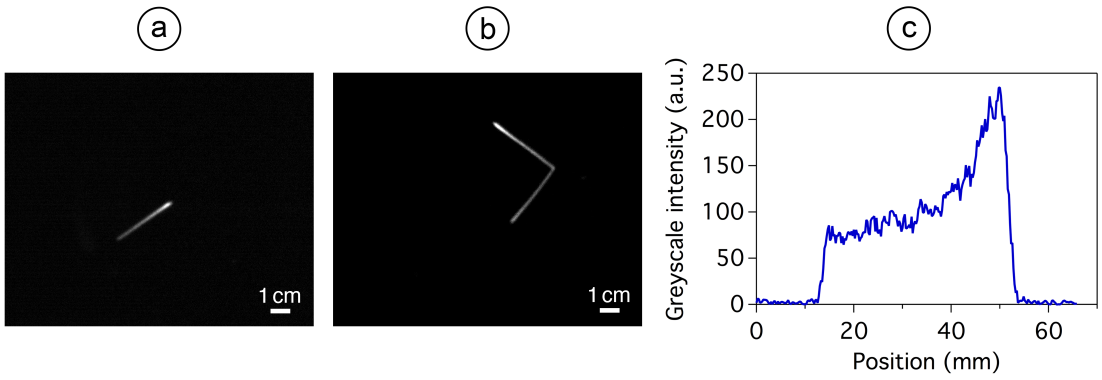

Figure 8. (a) Track of alpha particle originating from the decay of ^{220}Rn. (b) A second alpha particle is emitted during the subsequent decay of ^{216}Po to ^{212}Pb. (c) Line profile of grayscale values along the top alpha track shown in figure 8b. The Bragg peak can be clearly identified.

2018 JINST 13 T02006

Track profiles as shown in figure 8c can be used to visualise energy loss curves of the investigated particles. The unambiguous Bragg peak at the end of the particle track can be used to infer the direction of movement of the particle.

Augmenting the 2D projections of particle tracks with interaction depth information enables 3D track reconstruction based on optically read out images. In a Time Projection Chamber (TPC), depth information can be obtained from the arrival time of electrons at the endcaps [15]. In a GEM-based TPC, primary electrons originating from interactions closer to the cathode require more time to drift towards and reach the amplification structure used to read out a 2D projection at the endcap than primary electrons produced close to the GEM stack. Relative depth information between regions of a particle track can be extracted from the shape of waveforms from fast photon detectors such as PMTs or from electronically read out transparent multi-pad anodes. Absolute placement of 3D reconstructed tracks in the active volume of the detector requires depth of interaction information which can be obtained by detecting primary scintillation light produced during the initial ionisation processes in the drift volume by fast and highly sensitive photon detectors such as PMTs. A comparison of energy loss profiles obtained from PMT waveforms and optical images can be used to determine the orientation of particle trajectories. The possibility to combine the high position resolution provided by optical readout with depth information from fast photon detectors paves the way for optically read out GEM-based TPCs with high granularity readout of track projections at the endcaps.

3.4 Beam monitoring

Using gas as the target for radiation detection, low material budget detectors can be realised. Coupled with high granularity imaging sensors, inherent low sensitivity to electronic noise and prompt onscreen display of obtained images, optically read out gaseous detectors are well suited for beam monitoring applications in high energy physics or hadron therapy. Minimising material budget in the beam path, scintillation light emitted from a GEM during avalanche amplification can be coupled to a CCD or CMOS camera located outside of the beam path with a thin mirror. Using suitable materials, optically read out GEM-based detectors with a water equivalent thickness well below 1 mm for proton beams can be built. In the case of strongly ionising particle beams, single GEM amplification structures can be sufficient to emit enough secondary scintillation light to be detected with imaging sensors. For lower intensity or weakly ionising beams, multi-GEM amplification structures can be employed to reach amplification factors and consequently scintillation light intensities sufficient for optical readout.

A triple-GEM based detector read out with a CCD camera was placed in a pion beam to record the beam profile and the temporal evolution of the profile. High signal amplification factors allowed beam profile imaging with 8×8 pixel binning and an exposure time of 0.5 s. An integrated image of the pion beam profile obtained from a sum of images from 50 beam spills is shown in figure 9.

The visible structure outside of the main beam spot is mainly due to the movement of the beam spot during spills. This temporal evolution of the beam spot location during spills is attributed to beam delivery instrumentation inherent to the used beam line.

For beam profile monitoring of highly ionising, high intensity proton beams, a single GEM as amplification structure is sufficient to produce a copious amount of secondary scintillation light, allowing for even lower material budget in the beam path. A $10 \times 10\,\mathrm{cm}^2$ active area detector was

2018 JINST 13 T02006

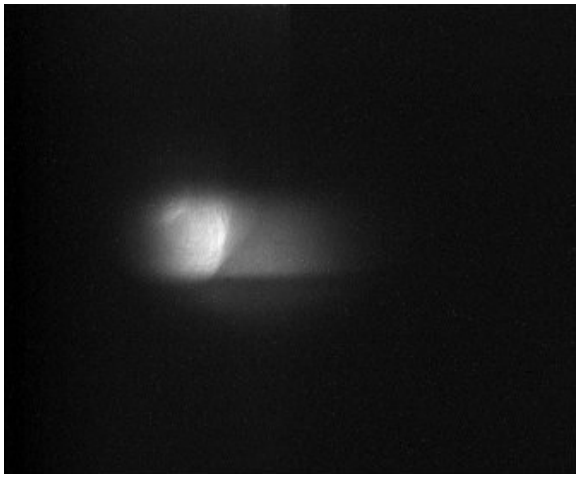

Figure 9. Integrated pion beam profile displaying movement of beam spot.

used to visualise the beam profile of a pencil proton beam as used in hadron therapy applications with energies ranging from 60 MeV to 226 MeV. Even low GEM gains below 10 were enough to record optically read out images of the beam profiles with exposure times on the scale of seconds. Pencil beam spots of 80 MeV and 226 MeV proton beams are shown in figure 10. The nominal decrease in beam spot width with increasing energy is accurately depicted in the obtained images and in horizontal line profiles across the centre of the beam spots as shown in figure 10c.

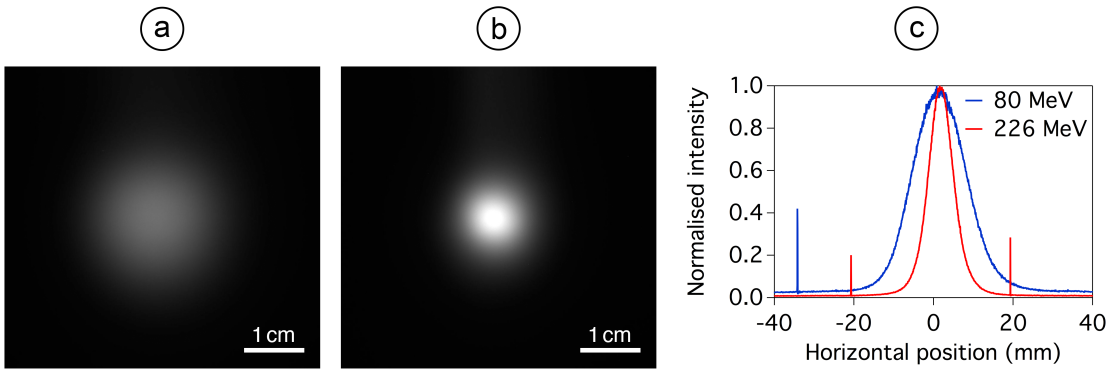

Figure 10. (a) Beam spot of 80 MeV proton beam. (b) Beam spot of 226 MeV proton beam. (c) Comparison of horizontal line profiles across the centres of beam spot images of 80 MeV and 226 MeV proton beams depict the nominal narrower beam profile for higher energy. Intensity spikes in the line profiles correspond to hot pixels resulting from direct interaction of radiation with the imaging sensor.

The frame rate of CCD or CMOS cameras coupled with the low material budget of gaseous detectors and the readily obtainable high scintillation light intensities allows for online beam profile monitoring detectors based on optically read out GEMs. Immediate optical representations onscreen without the need for time-consuming image reconstruction can be used for prompt reactions to changing beam parameters.

2018 JINST 13 T02006

4 Conclusion

Optical readout is an attractive alternative approach to the conventional electronic readout of MPGDs. Advances in imaging sensors have made high granularity sensors with low readout noise and good sensitivity readily available at reasonable cost. The high position resolution originating from the usage of CCD or CMOS cameras with a high pixel count and the inherent micrometer-scale structures of MPGDs make optical readout ideally suited for imaging applications. Direct image output without the need for extensive reconstruction algorithms enables real-time X-ray fluoroscopy and can be used in non-invasive material characterisation, radiation protection applications and functional medical imaging. Strong signal amplification by MPGD technologies such as GEMs allows for single low-energy X-ray photon sensitivity and consequently energy resolved imaging. Employing radially focused drift fields, parallax-induced broadening can be minimised in detectors with thick drift regions for increased detection efficiency enabling the usage of optically read out GEMs in X-ray fluorescence and crystallography applications. The high spatial resolution is also well suited for the readout of 2D particle track projections from the endcaps of TPCs. Combined with depth information from fast photon detectors, 3D particle track reconstruction is possible. The ability to immediately visualise events in the active volume of radiation detectors is one of the key advantages associated with optical readout as it allows real-time identification of the events and can be used for online monitoring purposes in radiation protection or beam profile monitoring applications. The wide range of ionising radiation detectable with MPGDs from MIPs to strongly ionising particles makes optically read out MPGDs a versatile tool for applications in fields ranging from high energy physics to radiotherapy and the low material budget of gaseous detectors makes them well suited for online beam profile monitoring.

Future advances in imaging sensors promise even greater numbers of high performance pixels providing even better position resolution with increased sensitivity. Although frame rates of current CCD and CMOS cameras are still relatively low and cannot be compared to readout speeds achievable with electronic readout, future developments might increase read out speed to a degree which enables the capture of multiple frames for single particle tracks enabling 3D reconstruction solely from acquired images. Combining microlens-arrays with CCD or CMOS cameras, plenoptic cameras can capture both intensity and direction of incident light rays and may at some point be used to directly obtain 3D trajectories of particles traversing suitable scintillating materials [16] or structures. Optical readout already features many advantageous characteristics for a wide range of applications and will further profit from technological developments in imaging sensors and camera technologies.

Acknowledgments

The authors gratefully acknowledge support in manufacturing the presented detectors by Christophe Bault (CERN, Geneva, Switzerland).

2018 JINST 13 T02006

References

[1] M. Titov and L. Ropelewski, *Micro-Pattern Gaseous Detector Technologies and RD51 Collaboration*, *Mod. Phys. Lett.* **A 28** (2013) 1340022.

[2] R.M. Gutierrez, E.A. Cerquera and G. Mañana, *MPGD for breast cancer prevention: a high resolution and low dose radiation medical imaging*, 2012 *JINST* **7** C07007.

[3] S.M. Larue and I.K. Gordon, *Radiation Therapy*, in *Withrow MacEwen's Small Animal Clinical Oncology*, Elsevier (2013).

[4] S. Andriamonje et al., *Experimental studies of a MicrOMEGAs neutron detector*, *Nucl. Instrum. Meth.* **A 481** (2002) 120.

[5] A.C. Stephan and L.F. Miller, *Micromegas neutron beam monitor neutronics*, *Radiat. Prot. Dosim.* **115** (2005) 357.

[6] F. Sauli, *GEM: A new concept for electron amplification in gas detectors*, *Nucl. Instrum. Meth.* **A 386** (1997) 531.

[7] M.M.F.R. Fraga, F.A.F. Fraga, S.T.G. Fetal, L.M.S. Margato, R. Ferreira Marques and A.J.P.L. Policarpo, *The GEM Scintillation in He-CF_4, Ar-CF_4, Ar-TEA and Xe-TEA Mixtures*, *Nucl. Instrum. Meth.* **A 504** (2003) 88.

[8] A. Morozov, L.M.S. Margato, M.M.F.R. Fraga, L. Pereira and F.A.F. Fraga, *Secondary scintillation in CF 4: emission spectra and photon yields for MSGC and GEM*, 2012 *JINST* **7** P02008.

[9] M. Gai et al., *An Optical Readout TPC (O-TPC) for Studies in Nuclear Astrophysics With Gamma-Ray Beams at HIgS*, 2010 *JINST* **5** P12004 [arXiv:1101.1940].

[10] C. Deaconu et al., *Track Reconstruction Progress from the DMTPC Directional Dark Matter Experiment*, *Phys. Procedia* **61** (2015) 39.

[11] F.A.F. Fraga, L.M.S. Margato, S.T.G. Fetal, M.M.F.R. Fraga, R. Ferreira Marques and A.J.P.L. Policarpo, *Optical readout of GEMs*, *Nucl. Instrum. Meth.* **A 471** (2001) 125.

[12] QImaging Corporation, *Retiga R6*, (2016).

[13] S. Duarte Pinto, et al., *Making spherical GEMs*, 2009 *JINST* **4** P12006 [arXiv:0909.3544].

[14] F.M. Brunbauer et al., *The planispherical chamber: A parallax-free gaseous X-ray detector for imaging applications*, *Nucl. Instrum. Meth.* **A 875** (2017) 16.

[15] D.R. Nygren, *The Time Projection Chamber: A New 4pi Detector for Charged Particles*, *eConf* **C740805** (1974) 58.

[16] F. Lebrun, R. Terrier, P. Laurent, C. Olivetto and E. Breelle, *US-9383457-B2-20160705*, US 9383457 B2 (2016).

2018 JINST 13 T02006